

Phase structure of non-Abelian lattice gauge theories

Claudio Rebbi

Department of Physics, Brookhaven National Laboratory, Upton, New York 11973

(Received 23 January 1980)

The phase structure of four-dimensional lattice gauge theories based on finite non-Abelian groups is studied by Monte Carlo computations. All models examined exhibit a two-phase structure with a first-order phase transition. In three systems where the gauge group is a discrete subgroup of $SU(2)$ the critical temperature moves toward zero as the order of the group increases and the high-temperature phase has confining properties.

I. INTRODUCTION

The lattice formulation of a gauge field theory offers a very powerful technique to study its quantum properties.¹ It provides a regularization of the ultraviolet divergences and allows strong-coupling expansions. The continuum theory is recovered in the limit where the correlation length becomes infinite; it is therefore quite crucial to have a knowledge of the possible phase transitions. Thus, the charge-confining properties of non-Abelian gauge models are related to the absence of any phase transition: The confinement observed in the strong-coupling regime is believed to extend all the way to the zero-temperature limit, where one recovers the continuum system. On the contrary, the existence of free charges in quantum electrodynamics requires a phase transition, separating a strong-coupling, confining phase from a low-temperature, spin-wave phase in the corresponding lattice theory.

Very recently numerical methods based on the Monte Carlo technique have been used to obtain information about the phase structure of a variety of gauge models.²⁻⁵ The results have proven quite encouraging and agree nicely with the conclusions of other analyses, based on perturbative or semiclassical expansions.⁶⁻⁸ More specifically, in Refs. 2 and 3 Abelian gauge theories have been investigated, while in Refs. 4 and 5 the non-Abelian system with gauge group $SU(2)$ has been studied.

A remarkable feature of lattice gauge theories is that discrete gauge groups may also be considered.⁹ Thus, together with the model with $U(1)$ gauge group, one may study the whole category of systems with the finite, Abelian groups Z_N . In the limit $N \rightarrow \infty$ one expects to recover the properties of the $U(1)$ theory. Indeed, one of the main results of the numerical analysis of

Ref. 3 consists in the observation, for N large enough, of a three-phase structure in the Z_N models, with two phase transitions, one of which disappears at zero temperature, while the other survives in the $U(1)$ limit. Considerations about this limit have also formed the main ingredient in the study of the Z_N models of Ref. 6.

The interrelations between the properties of lattice gauge theories with discrete and continuum groups motivated this work, where we present Monte Carlo results obtained for a variety of gauge systems with finite, non-Abelian groups. The main emphasis will be placed on models where the gauge group is a subgroup of $SU(2)$. Three of these systems, with gauge groups of 8, 24, and 48 elements, respectively, have been analyzed: All exhibit a single, very clear phase transition, which definitely moves toward zero temperature as the order of the group increases. Internal energy and disorder parameters (Wilson loop factors) of the high-temperature phase agree almost up to the transition point with those already determined for $SU(2)$.⁴

Contrary to the case of $U(1)$, the manifold of $SU(2)$ cannot be filled with points of discrete subgroups which become dense in a suitable limit. Only a finite number of nontrivial subgroups of $SU(2)$, related to the symmetries of the regular polyhedra, exists. But this is a limitation only in principle. We recall from Ref. 3 that the two phase transitions in the Z_N models are well separated already for $N=8$, with one transition essentially where it is observed in the $U(1)$ theory, the other at a temperature low enough to approach the limit of reliability of the computation. The model with a 48-element group considered here has the same energy (or action) gap as Z_8 (which is contained as a subgroup) and the only phase transition has already moved to a temperature lower than that for the Z_8 theory. Thus our results, we believe, corroborate strongly the notion

that four-dimensional lattice gauge theories with non-Abelian continuum groups possess a single, confining phase.

Section II contains a brief description of the models considered and of the computational technique used. Section III presents the actual numerical results. Section IV is devoted to a few words of conclusion.

II. DESCRIPTION OF THE MODELS AND OUTLINE OF THE COMPUTATION

A lattice gauge theory with group \mathfrak{g} is defined by associating an element $U_{ij} \in \mathfrak{g}$ to each link joining neighboring sites i and j . $U_{ji} = U_{ij}^{-1}$ and, in a gauge transformation, $U_{ij} \rightarrow U'_{ij} = G_i^{-1} U_{ij} G_j$, with the elements $G_i \in \mathfrak{g}$ defined locally at each site i . The quantities (Wilson loop factors)

$$W_\gamma = \text{Tr}\{U_{i_1 i_2} U_{i_2 i_3} \cdots U_{i_N i_1}\}, \quad (2.1)$$

where the sites i_1, \dots, i_N form a closed loop γ and Tr denotes a class function (i.e., $\text{Tr} G^{-1} U G = \text{Tr} U$), are gauge invariant.

In the applications to quantum field theory the lattice is usually taken to be a four-dimensional hypercubical lattice. Quantum averages are defined with a weight $e^{-\beta \mathfrak{s}}$, where the action \mathfrak{s} is given by a sum of suitable functions of loop factors extended to all elementary squares of the lattice (plaquettes)¹⁰:

$$\mathfrak{s} = \sum_{\square} f(W_{\square}). \quad (2.2)$$

Of particular interest are the normalization factor itself, or partition function,

$$Z = \sum_{\{U_{ij}\}} e^{-\beta \mathfrak{s}}, \quad (2.3)$$

the free energy, defined as

$$F = \frac{1}{N_s} \ln Z, \quad (2.4)$$

N_s being the number of sites in the lattice, which becomes independent of the lattice size as $N_s \rightarrow \infty$, and the internal energy

$$E = \langle f(W_{\square}) \rangle = \frac{1}{6} \frac{\partial}{\partial \beta} F. \quad (2.5)$$

In this article we shall study the models obtained with the following choices for \mathfrak{g} :

(i) The 8-element group of quaternions, denoted by Q , generated for instance by the matrices $i\sigma_x$ and $i\sigma_y$ (σ_i being the Pauli matrices).

(ii) The 24-element group \tilde{T} generated by the

matrices $\frac{1}{2} + \frac{1}{2}i\sqrt{3}\sigma_x$ and $\frac{1}{2} + (i\sqrt{2}/\sqrt{3})\sigma_y - (i/2\sqrt{3})\sigma_z$. T contains Z_2 as invariant subgroup and the factor group $T = \tilde{T}/Z_2$ is the rotation group of the tetrahedron.

(iii) The 48-element group \tilde{O} generated by the matrices $1/\sqrt{2} + (i/\sqrt{2})\sigma_x$ and $1/\sqrt{2} + (i/\sqrt{2})\sigma_y$. \tilde{O} also contains Z_2 as invariant subgroup and the factor group $O = \tilde{O}/Z_2$ is the rotation group of the octahedron.

(iv) The 24-element group O .

(v) The permutation group of three elements S_3 .

The groups Q , \tilde{T} , and \tilde{O} are subgroups of $SU(2)$. Their elements are represented by matrices of the form

$$u = \cos \vartheta + i \sin \vartheta \vec{\sigma} \cdot \hat{n}, \quad (2.6)$$

\hat{n} being a unit vector, and we choose $\cos \vartheta$ as the class function Tr appearing in Eq. (2.1). The action is then defined by

$$f(W_{\square}) = 1 - W_{\square}. \quad (2.7)$$

This agrees, in particular, with the normalization used in Refs. 2-4 and allows a direct comparison of results, without rescalings.

The elements of O may also be represented by matrices of the form (2.6), identifying however u with $-u$. W is then defined by $W = \cos^2 \vartheta$, as appropriate for the rotation group $O(3)$. $f(W_{\square})$ is again set equal to $1 - W_{\square}$.

The six elements of S_3 fall into three classes, one containing the identity I , another the two permutations of all 3 elements, C and C^2 , the third one the permutations P_i which leave the i th element fixed. I , C , and C^2 together form the invariant subgroup Z_3 and, to achieve the same normalization as in Ref. 3, we assign $f(W_{\square}) = 0$ to I , $f(W_{\square}) = \frac{3}{2}$ to C and C^2 . The choice of action for the remaining class is quite arbitrary and we have performed computations with the three values $f(\{P_i\}) = \frac{1}{2}$, 1, and $\frac{3}{2}$. Averages of loop factors have not been evaluated for this group, so the choice of W_{\square} itself is irrelevant.

The groups Q , \tilde{T} , and \tilde{O} are all subgroups of $SU(2)$, and one of the main purposes of this work is to study what happens to the phases of the corresponding gauge theories as the points representing the group elements become denser within the manifold of $SU(2)$. For comparison with the work of Ref. 3, we notice that \tilde{O} has subgroups isomorphic to Z_3 and, in particular, the gap between the action of an unexcited plaquette and the action of a plaquette in the lowest state of excitation is the same in both cases. O has been studied to see how factoring out the center of the group alters the properties of the model. S_3 has been con-

sidered for its own sake, also because the numerical analysis could be extended to this system with a minimal cost in computing.

Quantum averages are evaluated numerically by the Monte Carlo technique: One generates a sequence of states Σ_i in such a way that a definite configuration of the spin variables U_{ij} appears with a probability proportional to the Boltzmann factor:

$$P(\Sigma) \propto e^{-\beta S(\Sigma)}. \quad (2.8)$$

The quantum average of an operator $A(\Sigma)$ is then approximated by an average over configurations in the sequence

$$\langle A \rangle \approx \frac{1}{N} \sum_{i=0}^{i_0+N-1} A(\Sigma_i). \quad (2.9)$$

A number of states encountered at the beginning of the sequence is excluded to ensure that statistical equilibrium has been reached.

The configuration Σ_{i+1} is obtained from Σ_i by a stochastic process, whereby one of the spins of the lattice U_{ij} is set to a new value U'_{ij} (possibly equal to U_{ij}) according to a definite probability matrix $p(U_{ij} \rightarrow U'_{ij})$. p is defined so that in statistical equilibrium Eq. (2.8) is satisfied. After U_{ij} , a new spin U'_{ij} is reset according to p , and so on until all the spins of the lattice are probed in succession. This completes one Monte Carlo iteration. The whole process is then repeated and many iterations are used to construct the sequence of states appearing in Eq. (2.9). We refer the reader to Refs. 11 and 2-5 for a more detailed discussion of the method.

The matrix $p(U_{ij} \rightarrow U'_{ij})$ used in this analysis is constructed as follows. For all possible choices U'_{ij} the total action $S'(U'_{ij})$ of the plaquettes containing the link ij is evaluated. Then p is chosen proportional to $e^{-\beta S'(U'_{ij})}$:

$$p(U'_{ij}) = e^{-\beta S'(U'_{ij})} / \sum_{U'_{ij}} e^{-\beta S'(U'_{ij})}. \quad (2.10)$$

The statistical process thus corresponds to touching the spin U_{ij} with a heat reservoir at inverse temperature β , all other spins being held fixed. The procedure generated by this choice of p has been called the heat-bath algorithm in Refs. 2-4.

An alternative possibility for p , originally introduced by Metropolis *et al.*¹² and widely used, consists of selecting only one new candidate value U'_{ij} for the spin. If the new choice lowers the action, U_{ij} is changed to the new value. If not, the change is made with conditional probability $\exp[-\beta[s(U'_{ij}) - s(U_{ij})]]$. The computer time

needed to probe one spin with this algorithm is shorter than in the heat-bath method, but the heat-bath algorithm converges to statistical equilibrium faster (the relative efficiency depending on the number of possible values for the spins) and thus fewer Monte Carlo iterations are needed. In the context of the present analysis we found that the gain in convergence outweighs the loss in computer time and the heat-bath algorithm has been used throughout.

A technique of storing many spins in a single memory word of the computer (multi-spin-coding; see Ref. 2) to reduce memory requirements and processing time has been utilized. The computations have been performed with a lattice extending for 8 sites in each of the three spatial directions and 10 sites in the temporal one, subject to periodic boundary conditions but without any gauge constraint. The total number of spin variables is then 20 480, which, on the basis of previous results,²⁻⁴ should be sufficient to produce reliable averages without excessive statistical fluctuations.

III. THE PHASE STRUCTURE

While the basic feature of the Monte Carlo technique consists always in the stochastic readjustment of the spins, there are a variety of computations that can be done for a definite model. There is arbitrariness in the choice of the initial configuration; there is also the option of varying the parameter β every iteration or every few iterations, thus subjecting the system to a change in temperature. In a sense, the Monte Carlo algorithm creates a small specimen of the material inside the computer. But the choice of what experiment to do with it is left open.

In this study we have done the following three types of computation:

(i) Starting at a definite initial value β_0 of β (determined on the basis of trial computations) and with the system completely ordered (all U_{ij} set equal to the identity), 10 iterations are performed, the internal energy is evaluated, and β is lowered by an amount $\Delta\beta$. The procedure is repeated until β becomes zero (infinite-temperature limit) and then β is raised again, in steps of $\Delta\beta$, up to the original value β_0 . This computation, which we shall refer to as "simulation of a thermal cycle," provides a general overview of the phase structure of the system. The internal energy E is indeed a one-valued function of β (with the possible exception of a first-order critical point β_c where E can take two values, E_+ and E_-) so that in equilibrium a single value for the internal energy should be measured at any

definite temperature. By changing β , however, the system is constantly kept slightly off-equilibrium. If the variation of β is slow, the departure from equilibrium is generally very small and effectively a single value for E is determined. But near a phase transition the relaxation time becomes large and the plot of E versus β displays the typical shape of a hysteresis loop.

(ii) In the initial configuration half of the spins (those for instance emanating from sites with temporal coordinate ≤ 5) are set equal to the identity, the other half are chosen at random. A definite number of Monte Carlo iterations is then performed for a few fixed values of β , selected in the vicinity of a phase transition, and the internal energy E is plotted versus the number t of iterations. These computations, which we shall call "mixed-phase runs," provide information about the nature of the transition. At a critical point of the first order there are two different, stable phases. Slightly off the critical temperature one of the two phases remains stable, the other becomes metastable: In a mixed-phase run the system approaches rather quickly a configuration in which half the lattice is in the stable

phase and the other half is in the metastable phase, but then the boundary of the stable phase expands until this phase overtakes the whole lattice and one observes a drift in E towards either E_+ or E_- , according to the value of β . This behavior is qualitatively different from what is seen in a phase transition of higher order, where the curves $E(t)$ tend to equilibrium values which vary continuously when β is changed.

(iii) The loop factors W for rectangular paths of sides m and n are evaluated after equilibrium is reached at a definite temperature, averaging over all spacelike loops and also over a few Monte Carlo iterations. W plays the role of order parameter. Increasing the size of the loop the correlations among the spins decrease, W tends to zero and $-\ln W$ therefore to infinity.¹³ It has been argued that $-\ln W$ should increase like the area of the loop in a disordered, confining phase, like the perimeter in a nonconfining phase.¹ Thus, the behavior of $-\ln W$ versus m and n can be taken as a measure of the order of the system.

The thermal cycles for the models with groups Q , \tilde{T} , and \tilde{O} are reproduced in Figs. 1(a)–1(c). The range of temperatures has been covered in

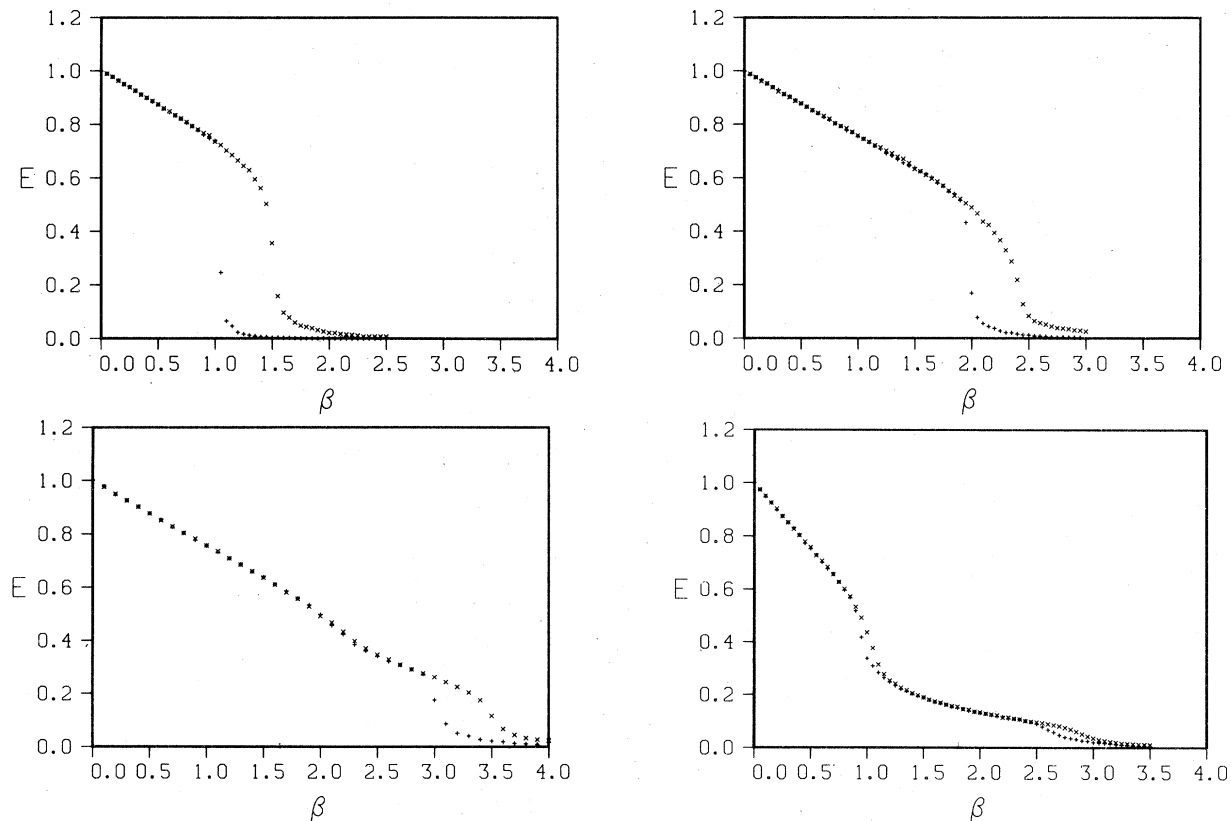


FIG. 1. Thermal cycles for the models with groups Q , \tilde{T} , \tilde{O} , and Z_8 . + (\times) denotes the values of E measured while increasing (decreasing) the temperature.

steps $\Delta\beta=0.05$ with the Q and \bar{T} systems, $\Delta\beta=0.1$ with the \bar{O} system. A hysteresis loop signaling a phase transition is apparent in all diagrams and it is also evident that the critical point moves toward zero temperature as the order of group increases: The groups Q , \bar{T} , and \bar{O} , we recall, are subgroups of $SU(2)$ with 8, 24, and 48 elements, respectively. The thermal cycle of the Z_8 model (from Ref. 3) is presented in Fig. 1(d) for comparison. The Abelian group Z_8 is contained as a subgroup in \bar{O} and the two models have the same energy (or action) gap. But the difference between their thermal cycles is impressive. The Abelian model gives clear evidence of two phase transitions and therefore of three phases: a high-temperature, confining phase,¹⁴ an ordered phase, likely to disappear at zero temperature when the order of the group increases, and an intermediate, nonconfining spin-wave phase. There is no sign of a spin-wave phase in the non-Abelian systems, and only the high-temperature, confining phase¹⁴ and the ordered, low-temperature phase appear to be present.

Mixed-phase runs have been made to determine the order of the phase transition and the critical temperature. Figures 2(a)–2(c) illustrate the

results of runs of 80 iterations with the Q , \bar{T} , and \bar{O} models, respectively. The values of β are indicated in the figure captions. Figure 2(d), presented for comparison, shows the result of a mixed-phase simulation with the Z_8 model near a critical point of higher order.³ In Figs. 2(b) and 2(c) a divergence of the curves $E(t)$ to limiting values E_+ and E_- is apparent. This trend is not so noticeable for the intermediate values of β in Fig. 2(a), but the results of longer runs, presented in Fig. 2(e), suggest a first-order transition for the system with gauge group Q as well. A longer run [see Fig. 2(f)] has also been done for the \bar{O} model to locate more precisely the critical point. These computations indicate that the systems with gauge group Q , \bar{T} , and \bar{O} all undergo first-order transitions, at critical temperatures given by $\beta_c=1.23\pm 0.02$, $\beta_c=2.175\pm 0.025$, and $\beta_c=3.21\pm 0.01$, respectively.

The behavior of the Wilson loop factors has been studied in the model with gauge group \bar{O} . Starting from an initial configuration where the system is in statistical equilibrium, averages of the loop factors have been taken over 12 Monte Carlo iterations and over all spacelike loops. For initial configurations we have chosen those encountered along the descending temperature

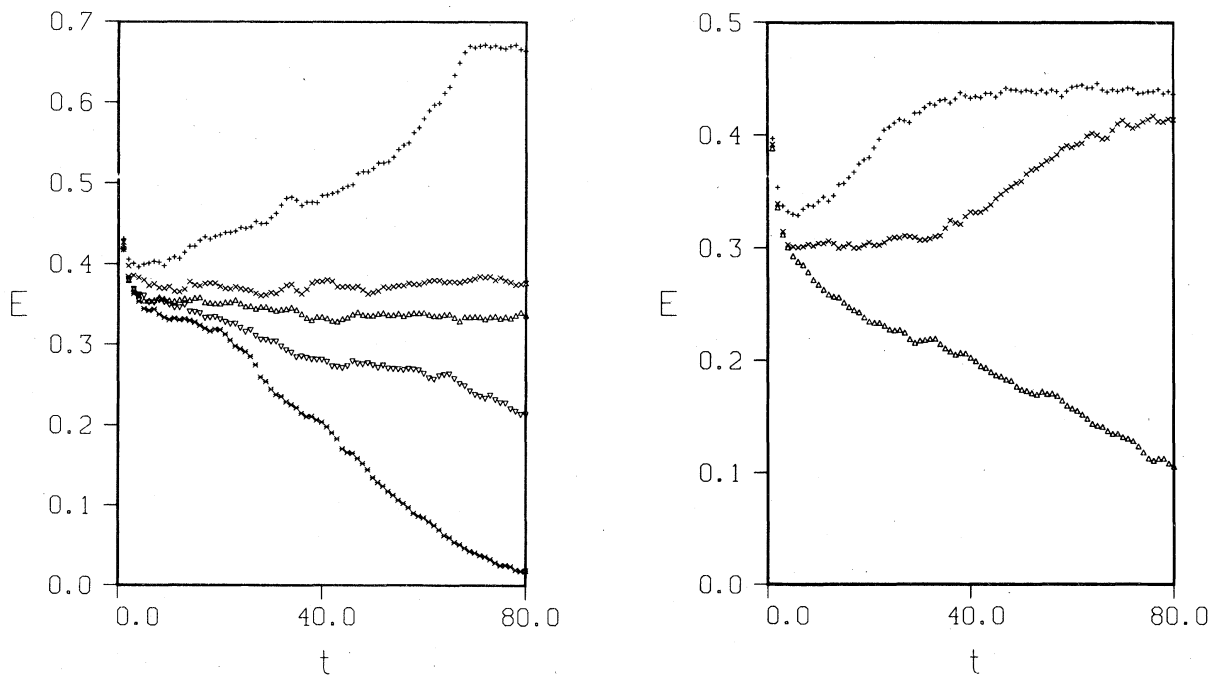


FIG. 2. Results of mixed-phase simulations. The models and temperatures are as follows: (a) Q ; $\beta=1.2(+)$, $1.23(\times)$, $1.25(\Delta)$, $1.27(\nabla)$, $1.3(*)$. (b) \bar{T} ; $\beta=2.1(+)$, $2.15(\times)$, $2.2(\Delta)$. (c) \bar{O} ; $\beta=3(+)$, $3.1(\times)$, $3.2(\Delta)$, $3.3(\nabla)$, $3.4(*)$, $3.5(\square)$, $3.6(\diamond)$. (d) Z_8 ; $\beta+0.97(+)$, $0.98(\times)$, $0.99(\Delta)$, $1(\nabla)$, $1.01(*)$, $1.02(\square)$, $1.03(\diamond)$. (e) Q ; $\beta=1.23(+)$, $1.25(\times)$, $1.27(\Delta)$. (f) \bar{O} ; $\beta=3.2(+)$, $3.22(\times)$, $3.24(\Delta)$.

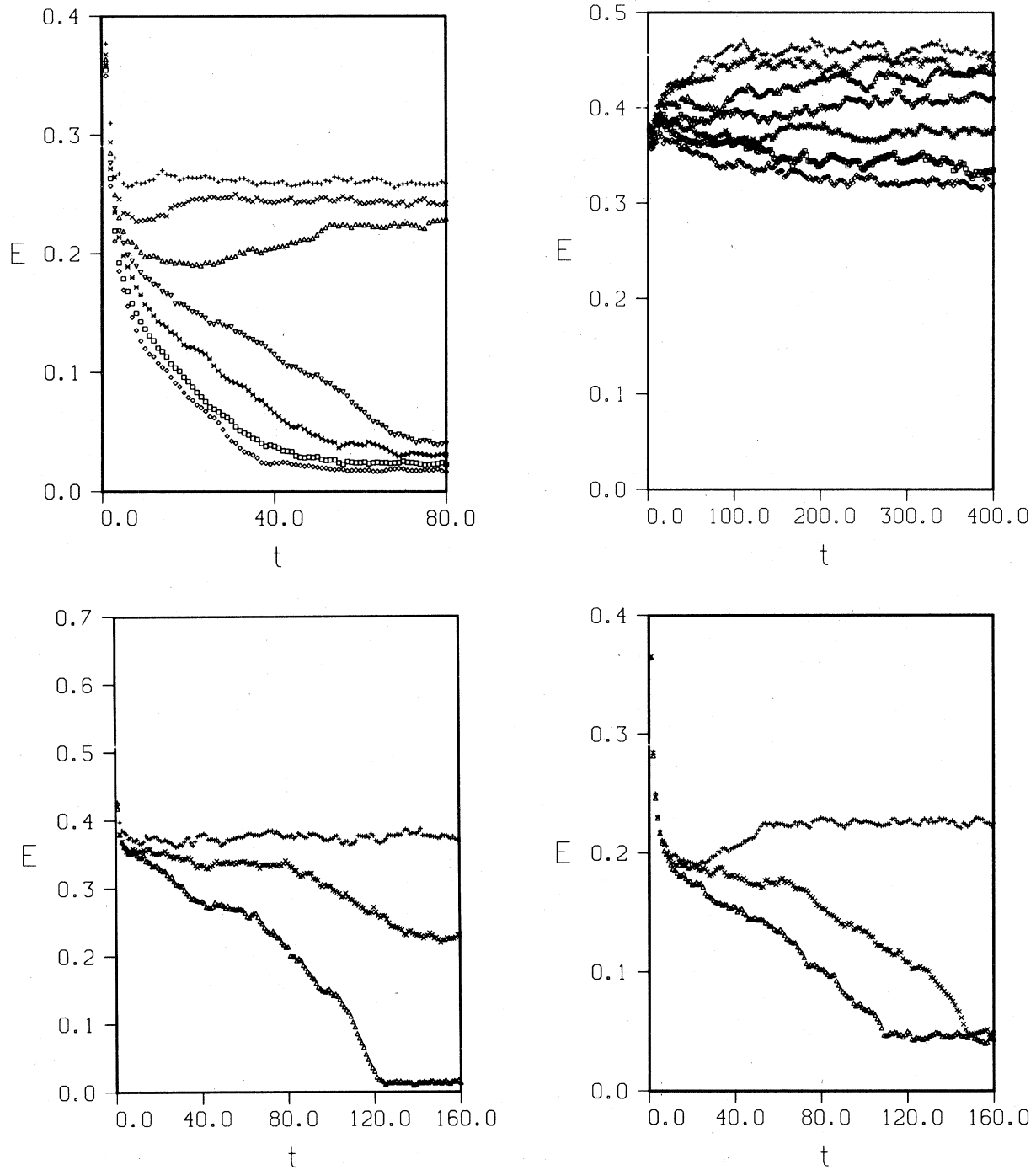


FIG. 2. (Continued)

branch of the thermal cycle for $\beta = 1, 1.5, 2, 2.5,$ and 3 ; those encountered at the end of the long mixed-phase runs (160 iterations) for $\beta = 3.2$ and 3.22 . In Table I we reproduce the values of $-\ln W$ thus determined for all the loops which give $-\ln W$

< 5 . Larger values of $-\ln W$ correspond to loop factors so close to zero that they cannot be distinguished from statistical fluctuations. These statistical fluctuations, not reported in the table, are of the order of 10^{-2} , with the exception of the

lowest temperature ($\beta=3.22$), where they are smaller.

From the table it is apparent that $-\ln W$ increases with the area of the loop in the high-temperature phase, whereas it is area independent in the low-temperature phase. This behavior becomes particularly manifest if one compares the values of $-\ln W$ for loops of the same perimeter and different areas, such as are found along the diagonals.

A quantitative determination of the coefficient T in the area term, or string tension, may also be attempted, but finite-size effects introduce some degree of ambiguity. Indeed, loops of size one and two are very likely too small for a measurement of the size dependence of the loops (they tend to give a larger area term, when inserted in a fit); on the other hand, as the loops approach the size of the lattice, increased correlations due to the periodic boundary conditions tend to make $-\ln W$ smaller ($-\ln W$ would be exactly zero for square loops of side eight in an Abelian system). Thus, for instance, for $\beta=2.5$ comparison of

loops measuring 3×3 and 4×2 gives $T=0.20$, comparison of loops measuring 4×4 and 5×3 gives $T=0.17$, a fit to the square loops of sides 1, 2, and 3 gives $T=0.145$, a fit to those of sides 2, 3, and 4 gives $T=0.075$. In spite of this degree of uncertainty, the computation reveals clearly a confining behavior of the high-temperature phase, with a disorder parameter T which decreases for increasing β , has a discontinuity at the phase transitions, and vanishes in the low-temperature phase.

Simulations of thermal cycles and mixed-phase runs have been done for the models with gauge groups O and S_3 . The results are displayed in Figs. 3 and 4. $\Delta\beta=0.05$ for all thermal cycles. The three cycles for the S_3 model correspond to different choices of the action to be associated with the odd permutations P_i .

All thermal cycles show hysteresis loops. In the S_3 model, as one might expect on general scaling considerations, lowering the action $f(\{P_i\})$ has the effect of increasing the value of β where the loop appears. The mixed-phase runs

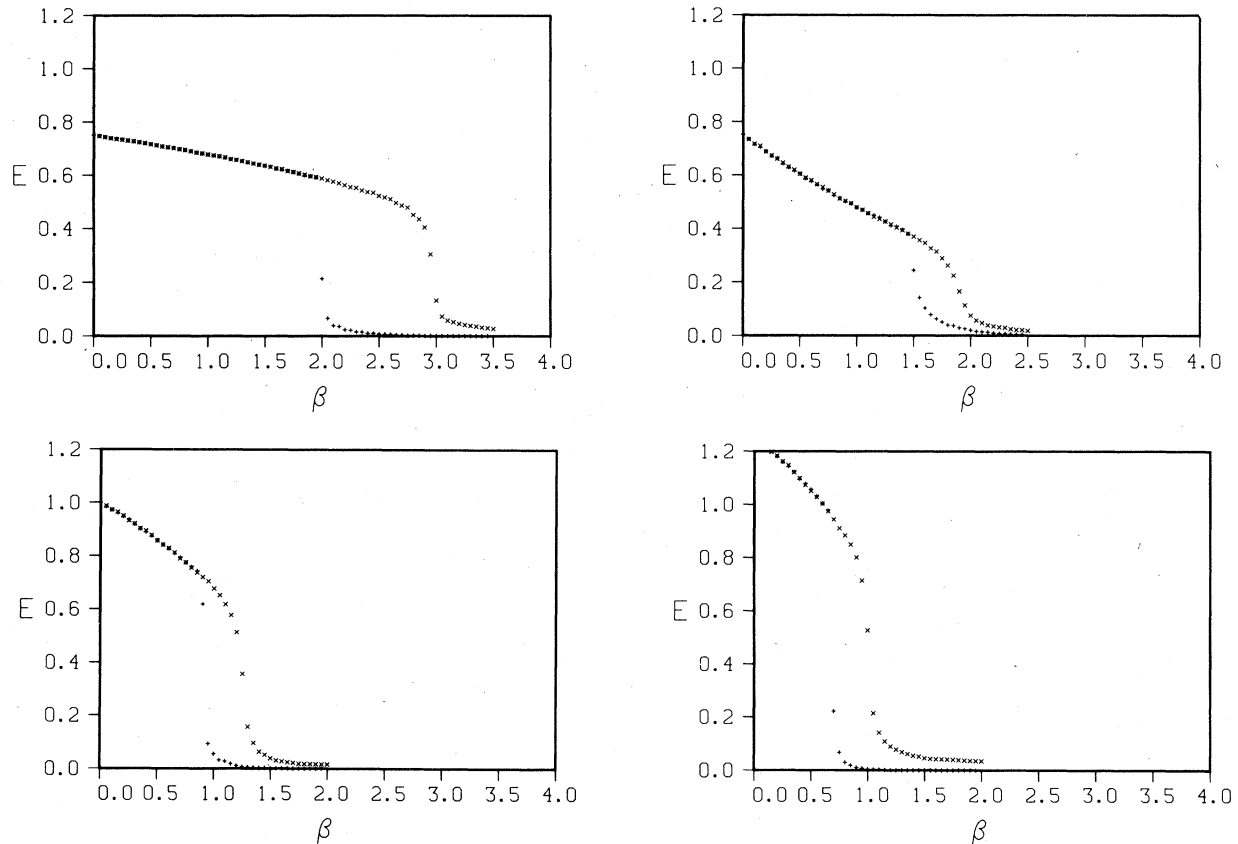


FIG. 3. Thermal cycles for the models with group O (a), and S_3 for three different choices of action: $f(\{P_i\})=\frac{1}{2}$ (b), 1 (c), and $\frac{3}{2}$ (d).

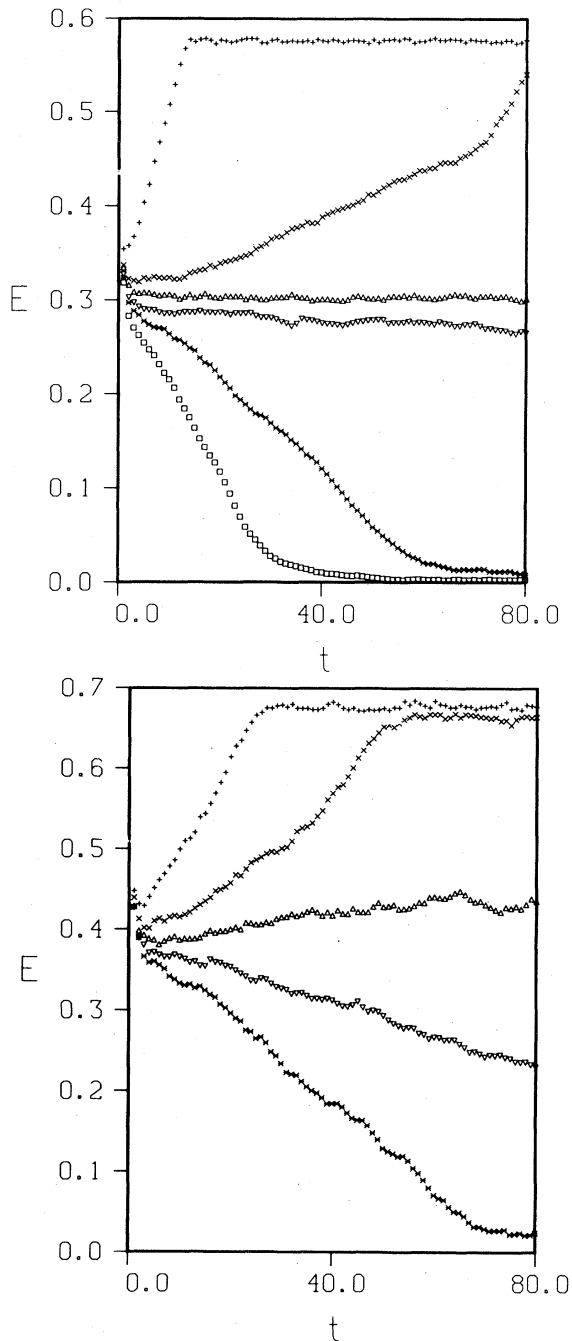


FIG. 4. Results of mixed-phase simulations for the O model and the S_3 model with $f(\{P_i\})=1$, respectively. The values of β are as follows: (a) $\beta=2.1(+)$, $2.3(\times)$, $2.4(\Delta)$, $2.5(\nabla)$, $2.6(*)$, $2.8(\square)$. (b) $\beta=1(+)$, $1.03(\times)$, $1.05(\Delta)$, $1.07(\nabla)$, $1.1(*)$.

[done only for $f(\{P_i\})=1$ in the S_3 model] indicate that the transitions are of the first order. The two intermediate curves in the O model diverge very slowly, but this may be attributed to the

temperatures being very close to the critical temperature. The behavior of the other curves is rather typical of a first-order phase transition.

IV. CONCLUSIONS

Our results give numerical evidence that all non-Abelian models considered have a two-phase structure with a first-order phase transition. In the three systems where the gauge group is a subgroup of $SU(2)$ the critical point definitely moves toward zero temperature as the order of the group increases. The analysis of the Wilson loop factors done for the \tilde{O} model, moreover, shows that the high-temperature phase is confining, with a string tension that becomes discontinuously zero at the critical point.

Very much as the phase structure of the Z_N models is suggestive of that of the system with gauge group $U(1)$, this study strongly supports the notion that a single, confining phase should be present in the model with gauge group $SU(2)$. We have compared our results for the \tilde{O} model with those obtained by Creutz⁴ for the $SU(2)$ model. The values found for the internal energy in the two different systems are displayed in Fig. 5: The agreement almost up to the critical β is impressive. We notice that the confining phase of the \tilde{O} system extends well beyond the value of β where Creutz finds a transition between the strong-coupling regime and the behavior predicted by asymptotic freedom⁴ or where instanton contributions are detected;⁸ thus already with the finite gauge group one finds confinement throughout the region where one would expect the most interesting effects to take place.

The values $-\ln W$ found in Ref. 4 for the square loops also agree well with those we find for the \tilde{O} model (for $\beta < \beta_c$). For instance, Creutz finds

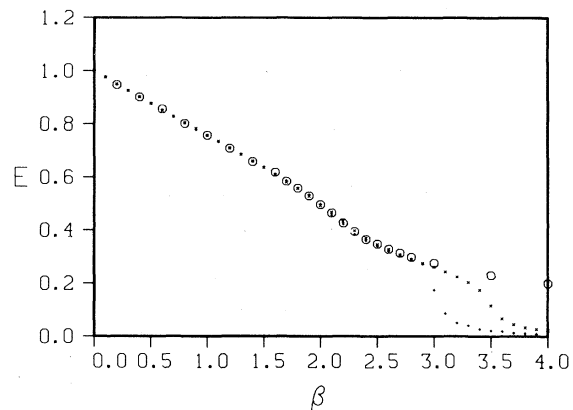


FIG. 5. Comparison of the internal energies of the systems with gauge group \tilde{O} (+ and \times) and $SU(2)$ (o).

values 0.43, 1.36, 2.46, and 3.50 for square loops of side 1, 2, 3, and 4 at $\beta=2.5$ to be compared with our values 0.42, 1.35, 2.57, and 3.94. This remarkable agreement between quantities measured in the two models suggests the interesting possibility of using the \tilde{O} model, or the model based on the 120-element subgroup of $SU(2)$, for reliable approximate computations of observables of the $SU(2)$ system itself. The saving in memory requirements and computing time could allow the study of larger lattices.

Our understanding of non-Abelian gauge systems has certainly progressed during the last few years. The hypothesis of confinement, that not

so long ago was a mere conjecture, is now strongly supported by a variety of numerical, perturbative, and semiclassical computations. The time may be ripe to promote the hypothesis into a theorem, with the rigor of analytical proof.

ACKNOWLEDGMENTS

I gratefully acknowledge the participation of Laurence Jacobs in early computations done for the system with gauge group Q . This research was performed under Contract No. DE-AC02-76CH00016 with the U.S. Department of Energy.

-
- ¹K. G. Wilson, *Phys. Rev. D* **10**, 2445 (1974).
²M. Creutz, L. Jacobs, and C. Rebbi, *Phys. Rev. Lett.* **42**, 1390 (1979).
³M. Creutz, L. Jacobs, and C. Rebbi, *Phys. Rev. D* **20**, 1915 (1979).
⁴M. Creutz, *Phys. Rev. Lett.* **43**, 553 (1979); *Phys. Rev. D* **21**, 2308 (1980).
⁵K. G. Wilson, Cornell University report, 1979 (unpublished).
⁶S. Elitzur, R. B. Pearson, and J. Shigemitsu, *Phys. Rev. D* **19**, 3698 (1979); D. Horn, M. Weinstein, and S. Yankielowicz, *ibid.* **19**, 3715 (1979); A. Ukawa, P. Windey, and A. Guth, *ibid.* **21**, 1013 (1980).
⁷J. Kogut, R. B. Pearson, and J. Shigemitsu, *Phys. Rev. Lett.* **43**, 484 (1979).
⁸C. G. Callan, R. Dashen, and D. J. Gross, *Phys. Rev. D* **20**, 3279 (1979); *Phys. Rev. Lett.* **44**, 435 (1980).
⁹F. J. Wegner, *J. Math. Phys.* **12**, 2259 (1971); R. Balian, J. M. Drouffe, and C. Itzykson, *Phys. Rev. D* **10**, 3376 (1974); **11**, 2098 (1975); **11**, 2104 (1975).
¹⁰While with our definition $f(W_\square)$ is again a loop factor

with different class function Tr , later it will be convenient to assume a specific form for Tr in Eq. (2.1) and the elementary action is denoted $f(W_\square)$ for consistency.

¹¹K. Binder, in *Phase Transitions and Critical Phenomena*, edited by C. Domb and M. S. Green (Academic, New York, 1976), Vol. 5B.

¹²N. Metropolis, A. W. Rosenbluth, M. N. Rosenbluth, A. H. Teller, and E. Teller, *J. Chem. Phys.* **21**, 1087 (1953).

¹³Up to boundary effects. The periodic boundary conditions introduce correlations when the size of the loop becomes close to extent of the system in the spatial directions and eventually a decrease in $-\ln W$ is observed. For a square loop of side 8, W can still be different from 1 (the value it would take in an Abelian system) because of the noncommutativity of the U_{ij} .

¹⁴The evidence that the high-temperature phase has confining properties is obtained from the analysis of the loop factors, to be presented later for the \tilde{O} model and discussed in Ref. 3 for the Z_N models.